Peer-reviewed version available at Processes 2019, 7, 710; doi:10.3390/pr7100710

Article

Hydrodynamic and Hydrographic Modeling of Istanbul Strait

Mehmet Melih Koşucu [1]*, Mehmet Cüneyd Demirel [1], V.S. Ozgur Kirca[1] and Mehmet Özger [1]

[1] Istanbul Technical University, Civil Engineering Faculty, Hydraulics Division; kosucu@itu.edu.tr, demirelmc@itu.edu.tr, kircave@itu.edu.tr, ozgerme@itu.edu.tr

* Correspondence: kosucu@itu.edu.tr;

Abstract: The aim of this study is to model hydrodynamic processes of the Istanbul Strait with its stratified flow characteristic and calibrate the most important parameters using local and global search algorithms. For that two open boundary conditions are defined, which are in the North and South part of the Strait. Observed bathymetric, hydrographic, meteorological and water level data are used to set up the Delft3D-FLOW model. First, the sensitivities of model parameters on the numerical model outputs are assessed using PEST toolbox. Then, the model is calibrated based on the objective functions focusing on the flowrates of upper and lower layers. The salinity and temperature profiles of the Strait are only used for model validation. The results show that the calibrated model outputs of Istanbul Strait are reliable and consistent with the in-situ measurements. The sensitivity analysis reveals that the Spatial Low-Pass Filter Coefficient, Horizontal Eddy Viscosity, Prandtl-Schmidt Number, Slope in log-log Spectrum and Manning Roughness Coefficient are most sensitive parameters affecting flowrate performance of the model. The agreement between observed salinity profiles and simulated model outputs is promising whereas the match between observed and simulated temperature profiles is weak showing that the model can be improved particularly for simulating the mixing layer.

Keywords: Istanbul Strait; stratified flow; gravity driven flow; numerical modelling

1. Introduction

Istanbul Strait is one of the most prominent straits in the World. Due to the constructional, navigational and deep see discharge activities, understanding the flowrates of the Istanbul Strait bears importance. The Strait connects Black Sea (in the North) and the Marmara Sea (in the South) providing continuous water exchange between these two water bodies. For centuries, the hydrodynamical and hydrographical structure of the Strait has been the subject of many research efforts and broad discussions dating back to centuries ago.

Çeçen et al. [1] made observations, and established a mathematical model of the Istanbul Strait. Salinity and temperature profiles of Istanbul Strait are visualized in 4 different seasons of 1980. Bayazıt and Sümer [2], in a continuation of Çeçen et al.'s study, reported the salinity and water mass balance equations. Results of these studies agreed with observations. Sumer and Bakioğlu [3], proposed a one-dimensional mathematical model utilizing the observations from Anadolu Kavağı (North) and Üsküdar (South) stations. Sumer and Bakioğlu [3] stated that water level variations between two sides of the Strait have a strong impact on the stratified flow structure. Latif et al. [4] asserted that the density-driven lower layer flow in the Strait could not reach the Black Sea from time to time, especially when the strong Northerly winds blow. These winds, generating a significant shear force on the Strait, could blockade the lower layer flow such that it could not continue towards Black Sea direction. In addition, when the river discharges into the Black Sea increases, freshwater entrance to the Strait rises. Water level rising in the Black Sea can also blockade lower layer flow [5]. Falina et

al. [6] ascertained that “Mediterranean Originated Water” intruded to Black Sea’s 100-600 m depths through Istanbul Strait during strong cyclonic storms.

Sur et al. [7] indicated that the Danube River's impact on Black Sea water level was much stronger than the other rivers flowing into the Black Sea. When the Danube River’s flowrate rises, an increment on the discharge of upper layer flux of the Strait occurs. Oğuz et al. [8] established a mathematical model, and stated that there were three control zones termed as "Hydraulic Controls" of the Strait. Two of these are located in the Northern and Southern parts of the Strait (two silled zones), whereas the third is the narrowest section of the Strait. These zones are significant for the hydrodynamics of the Strait since “Maximal Exchange" events occur in these locations [9], [10], [11]. This events are characterized with the enhanced mixing between the lower and upper layers of the Strait. Dorrell et al. [12] mentioned the “internal hydraulic jump” in the Istanbul Strait, which occurs in the Hydraulic Control sections. As very well known, during the normal hydraulic jump, Froude Number becomes near to unity while the flow regime switches from subcritical to supercritical. However, it could be said that there is no critical value of stratified depth-averaged Froude Number, on the contrary of Normal Hydraulic Jump. Beşiktepe et al. [13] made observations, and conducted measurements with ADCP and CTD devices in the Turkish Straits. Based on these activities, salinity, temperature, and current velocity profiles were developed. Özsoy et al. [14] executed current velocity and flowrate measurements in the Turkish Straits, and consequently described the structure of Istanbul Strait as outstanding because of its maximal exchange issue. Gregg et al. [15] stated that the flow condition of the Strait is at "Quasi-Steady State". Gregg and Özsoy [16] expressed opinions about this "Quasi-Steady State" flow conditions. According to these considerations, when upper layer flow enters the Marmara Sea, and lower layer flow enters the Black Sea, flow regimes are supercritical. Moreover, bottom friction is required to evaluate the hydrodynamic structure of the Strait. Güler et al. [17] made long-period velocity measurements at various points in the Istanbul Strait. The measurements were conducted between May and September of 2003, which represent the hydrodynamic condition of the summer season. Yüksel et al. [18] built up velocity profile of the Strait, and asserted that current regime of the Strait was evaluated from wind and atmospheric pressure, as well as fresh water from rivers discharging into the Black Sea. Aydoğan et al. [19] modeled the current velocities of the Strait with Artificial Neural Networks (ANN) method. In the mentioned study, the advantages and disadvantages of the ANN method were evaluated accurately about the prediction of Istanbul Strait’s current velocity. Jarosz et al. [20] commented on ADCP and CTD data in the Strait between September 2008 and February 2009. Altiok and Kayışoğlu [21] executed current velocity, temperature and salinity measurements with ADCP and CTD devices during 11 and 15 years, respectively. Even if some certain mean values were given for upper and lower layer fluxes, the flux values differed from North to South [22]. Because of maximal exchange phenomena in the Hydraulic Control sections, upward entrainment fluxes from the lower layer to upper layer increase the upper layer flowrate. Therefore, upper layer flowrate values are generally larger in the North section of the Strait compared to the South.

Akay [23] proposed a numerical modeling study of the Istanbul Strait conducted with Telemac3D software. In that study, an unstructured grid and finite element method were used. Akay took the Southern boundary conditions as discharge values which are osculated to study of Özsoy et al. [14], and Northern boundary conditions as free-water level and current velocity values. Öztürk [24] established a numerical model of the Strait with an unstructured grid, which was based on the finite volume method with MIKE 3 software. Water level, salinity and temperature values were estimated as boundary conditions. After the running of the model, it was observed that measured and modeled current velocity values were in accordance. Sözer [25], and Sözer and Özsoy [26] numerically modeled Istanbul Strait by use of the ROMS (Regional Ocean Modeling System) software, which was based on the finite volume method. For Black Sea boundary conditions, Şile water level measurements were used, and for Marmara Sea boundary conditions Yalova water level measurements were input. Salinity and temperature boundary conditions were entered as constant with depth and stratification was maintained. It was concluded that stratified boundary transport conditions lead to realistic consequences in the model. Sannino et al. [27] established a hydrodynamic

Peer-reviewed version available at Processes 2019, 7, 710; doi:10.3390/pr7100710

model of the whole Turkish Straits. In this study, Özsoy et al.'s [14] measurements, Sözer's [25] Istanbul Strait model results, and the whole Turkish Straits System's (TSS) model results were compared. According to Sannino et al's [27] study, the whole TSS model represents an accordance with the in-situ observations. Strait of Gibraltar presents another two-layered dynamic system which is similar to Istanbul Strait [28]. Except the tidal dynamics, modeling the Strait of Gibraltar bears affinity with modeling Istanbul Strait [29]. Although there have been many studies conducted to solve the hydrodynamics and/or hydrography of this sophisticated two-layer system, none of the previous studies focused on the sensitivity of the results against the input parameters used in the model. Furthermore, unlike many of the previous studies, the present study facilitates a direct comparison of numerical modeling results with the in-situ hydrographic data, namely salinity and temperature profiles along the Istanbul Strait.

In the present study, a numerical hydrodynamic model of Istanbul Strait is established using the DELFT3D-FLOW, which is a open source hydrodynamic simulation software utilizing finite differences method and a structured grid system [30]. The objective of the study is two folds; (1) to assess the sensitivity of the flow regime against different input parameters in order to select most important parameters for the calibration and (2) to calibrate the model using local and global algorithms to simulate both the hydrodynamics and hydrography of the two-layer flow system. To represent the real conditions occurring in the Strait, the proposed model was calibrated against flowrates of the upper and lower layers, and tested using the salinity and temperature measurements. With the numerical results, the hydrodynamics of the stratified flow in the Istanbul Strait is evaluated.

2. Materials and Methods

The uniqueness of physical and hydrodynamic characteristics of Istanbul Strait has attracted the interest of researchers for decades. The physical structure of the Istanbul Strait presents a natural channel shape, which is meandering, widening, narrowing, deepening, and shoaling. Net length of Istanbul Strait is 31 km. The maximum depth is 110 m, minimum depth is nearly 30 m, and the widest and narrowest sections are 3500 m and 700 m in width, respectively (Figure 1).

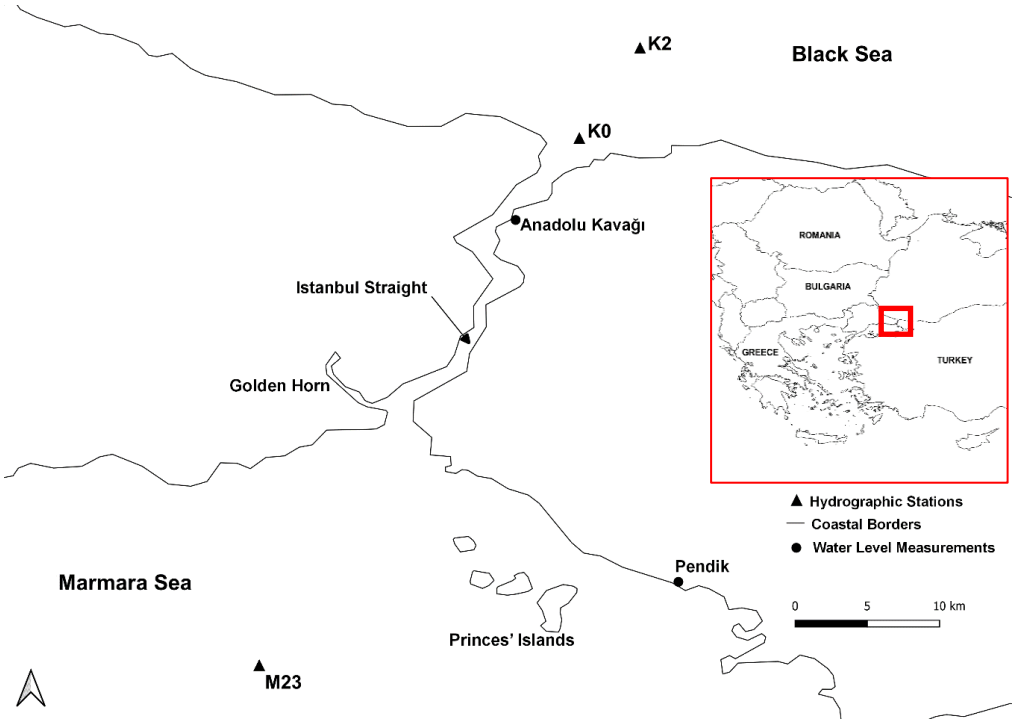

Figure 1. Study area and hydrographic observation stations in the Istanbul strait [31].

As mentioned above, the most significant feature of the flow in Istanbul Strait is that there are two different flows in the upper and lower layers in opposite directions. In Figure 2, the longitudinal section of the strait is given with a schematic representation of the flow structure. While the upper layer flow is towards North from the Black Sea to the Marmara Sea, the lower layer flow is towards South from the Marmara Sea to the Black Sea. Less salty (hence lighter) Black Sea water constitutes the upper layer of the Strait. Upper Layer is colder than the lower layer in winter months and warmer in the summer months. The lower layer is saltier than the upper layer, and coming from the Mediterranean Sea [4]. The intermediate (mixing) layer lies between the upper and lower layers and the thickness of this layer oscillates with the effect of internal waves.

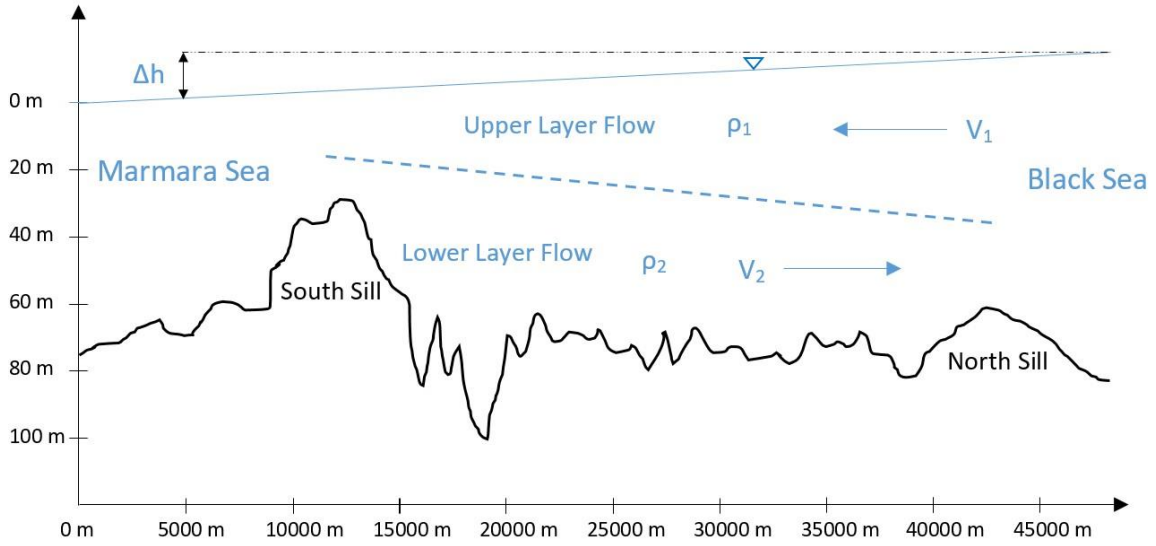

Figure 2. Schematic description of the longitudinal section of the Istanbul Strait based on [2]-.

For setting up a reliable numerical model, bathymetric, mareographic, hydrographic and meteorological data are essential. For the present study, bathymetric data was obtained from Turkish Navy Office of Navigation, Hydrography and Oceanography.

Water level differences between two sides of the Strait -which governs the hydrodynamic structure of the flow through the Strait- are used as input forcing in the model. For this purpose, mareographic data of the 2003 year was obtained from the Turkish Naval Forces. Southern and Northern boundaries of the Strait are represented by water level data of Pendik and Anadolu Kavağı stations, respectively, as shown in Figure 3.

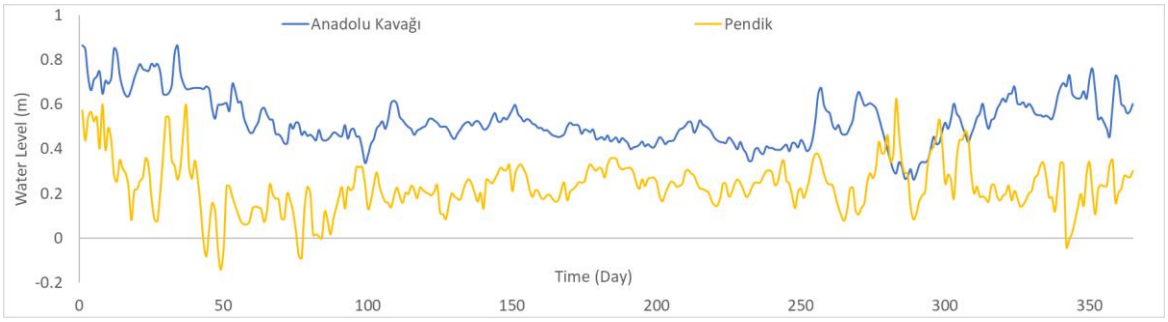

Figure 3. Daily water level values in Pendik and Anadolu Kavağı mareography stations in 2003.

As stated above, the main reason for the stratification of the Strait is the density variation by depth. Two main factors affecting density variation, salinity and temperature, are incorporated in the hydrodynamic model. Salinity and temperature variation data were taken from the ISKI (Istanbul Water and Sewerage Administration) hydrographic observation stations [31]. The stations K0 and K2

Preprints (www.preprints.org) | NOT PEER-REVIEWED | Posted: 28 August 2019 doi:10.20944/preprints201908.0299.v1

Peer-reviewed version available at Processes 2019, 7, 710; doi:10.3390/pr7100710

are selected for the Northern boundary, whereas the station M23 is chosen for the Southern boundary, which are shown in Figure 1. For two boundaries of the Strait, monthly observations of salinity and temperature data are used as input parameter in the model (Figure 4).

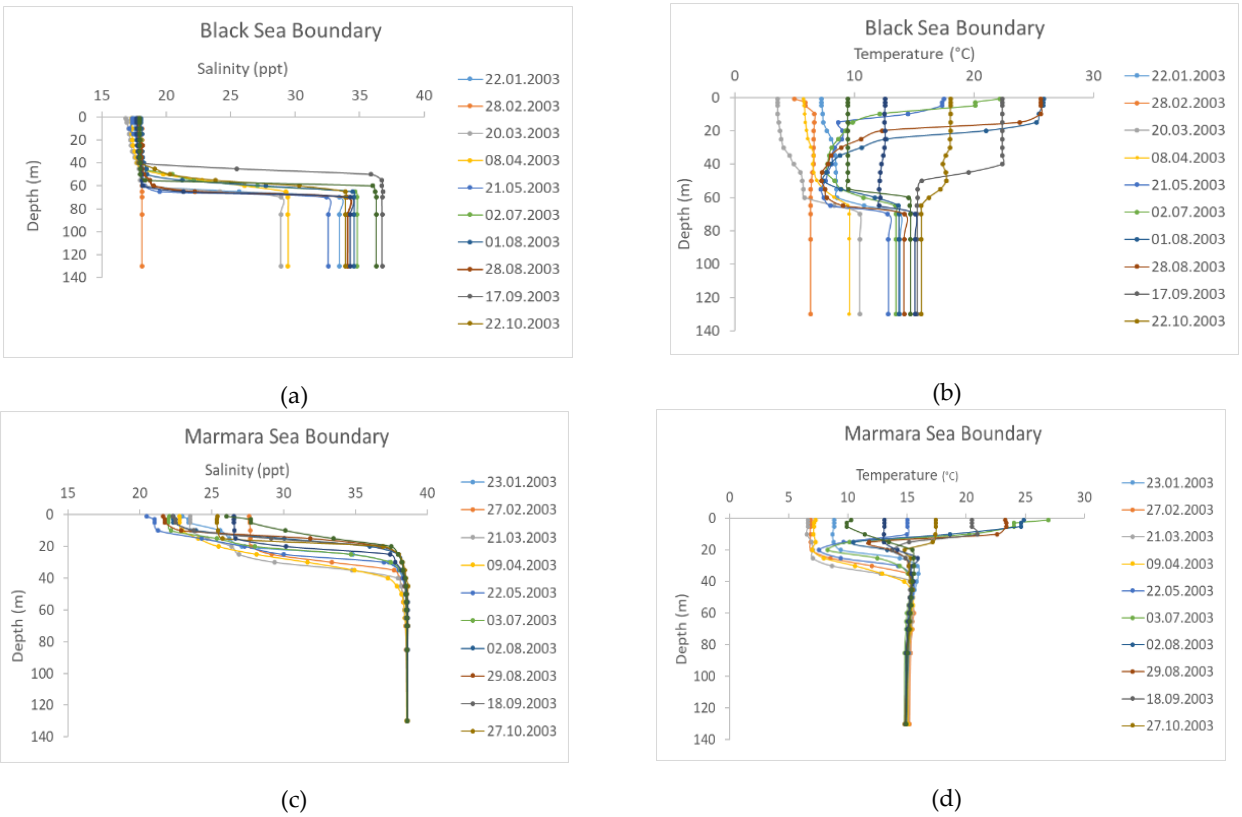

Figure 4. First row shows a) salinity in Black Sea b) temperature in Black Sea and second row shows c) salinity in Marmara Sea d) temperature in Marmara Sea boundaries of the Istanbul Strait.

For modeling the hydrodynamical structure of the Istanbul Strait, meteorological data is required to include the effect of atmosphere-sea interaction taking place at the near-surface part of the water mass, since wind shear and barometric differences are important flow forcing factors, as well as the water level and density differences. To serve as input data for the model, mean sea level pressure values, and wind velocity components u (direction in east-west) and v (direction in north-south) at 10 m altitude are obtained from ECMWF database.

2.1. Model Setup

The hydrodynamic model of the Istanbul Strait is established in Delft3D-FLOW. This model is based on finite element method and often used in hydrodynamical modeling of Coasts, Rivers, Estuaries, and Seas with governing equations of fluid dynamics [32]. These equations are the Navier-Stokes equations which also includes Reynolds stresses (RANS equations) with the k-ε closure. It should be noted that Delft3D-FLOW operates with hydrostatic pressure instead of solving the whole suit of RANS equations. Details can be found in [32].

To set up the hydrodynamic model in Delft3D-FLOW following steps are applied: (1) computational grid generation, (2) input of bathymetric conditions, (3) input of other parameter values, (4) initial conditions assignment, (5) boundary conditions assignment, and (6) selection of observation point the locations (locations for model output).

To simulate fluid motions, continuity and momentum equations (RANS equations) should be solved. However, these equations –especially momentum equations- are in the form of non-linear partial differential equations. Since these equations are non-linear, it is not possible to solve them analytically. Numerical finite difference method is used to approach the exact solution of these

equations in a computationally-efficient manner. The computational grid, which is an important part of the solution scheme, was generated by discretizing the flow domain using the RGFGRID module of Delft3D. In the model, horizontal and vertical grids were used. The horizontal grid facilitates the representation of the fluid motions throughout the Strait in the North-South direction (Figure 5a). Horizontal Grid domain used in the model covers the region between 30.0354 and 28.0944 longitudes and 41.4756 and 40.7878 latitudes. Total horizontal grid cell quantity is 685. Maximum and minimum grid lengths are 6161 m and 198 m, respectively. Coarse (≈ 6000 m) section of the computational grid, corresponds to open sea zones. The grid spacing gets finer inside of Istanbul Strait for maintaining the computational efficiency as well as computational accuracy.

Vertical grid is also important to observe the stratification effect. Unlike many of previous research [33] [34] [35], z-model was used in this study in favor of σ-model, meaning that the number of grid cells in the vertical were not constant but variable as a function of depth. This is because, z-model is known to be more capable to accurately model stratified flow conditions [32]. As shown in Figure 5b, the vertical grid lines are perpendicular. Nevertheless, perpendicularity of grids is distorted occasionally, especially in near-bottom regions. But in the Intermediate Layer, perpendicularity is intact and avails stratification of the flow field. All vertical grid lengths are taken as constant at 5 m.

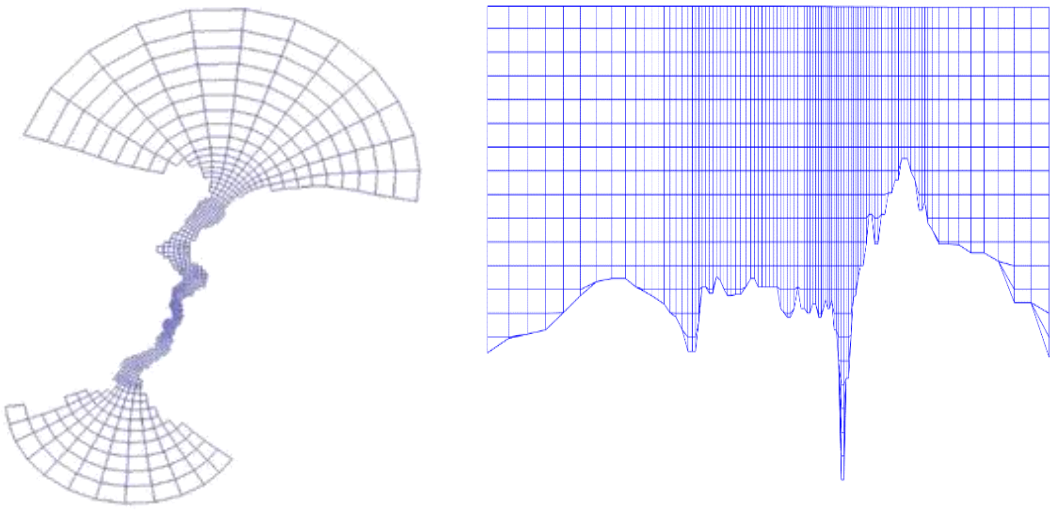

(a) (b)

Figure 5. Hydrodynamic Grid of the Model (a) vertical and (b) horizontal directions

Bottom topography of the Strait exhibits an irregular and variable shape. Figure 6 shows the point-based (raw data) and refined area based bathymetry. Refined bathymetry is established in QUICKIN module of Delft3D by triangular interpolation method. This way a more realistic bathymetric boundary condition can be achieved.

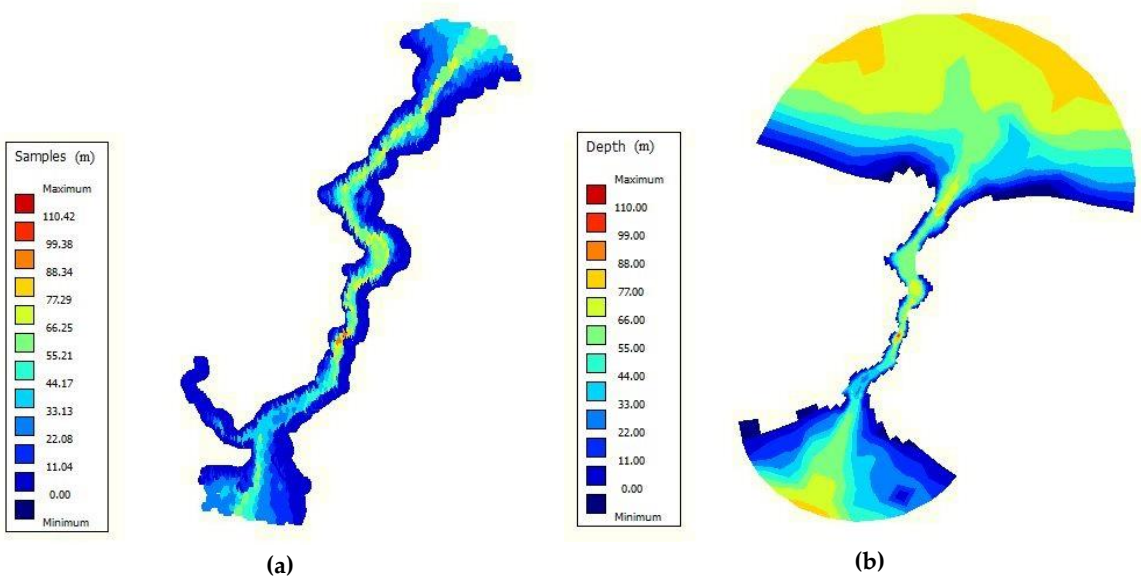

198 Figure 6. Point-based (raw) (a) and area-based (refined) bathymetry data of the Strait (b)

199 There are several other input parameters in the model such as time-related parameters,
200 roughness, viscosity and turbulence parameters. Time-related parameters include the time domain
201 and time step parameters. Time domain of the numerical run starts at 01.01.2003 – 00:00:00 and
202 finishes at 01.01.2004 – 00:00:00. Time step is chosen as 0.25 minutes (15 seconds) i.e. small enough to
203 accurately capture the unsteady behavior of the flow. Five of the input parameters: (1) Manning
204 Roughness Coefficient, (2) Horizontal Eddy Viscosity, (3) Slope in Log-Log Spectrum, (4) Prandtl-
205 Schmidt Number, and (5) Spatial Low-Pass Filter are designated as calibration parameters. Vertical
206 eddy viscosity and diffusivity parameters are 10^{-4} m^2/s and 10^{-5} m^2/s [32]. As mentioned above, k-$\boldsymbol{\varepsilon}$
207 Turbulence Model is selected in the model.
208 Water level values at both ends of the Strait were chosen for the hydrodynamic open-boundary
209 conditions. Like mentioned above, as the Northern boundary conditions, Anadolu Kavağı water level
210 data (Figure 3), and as the Southern boundary conditions, Pendik water level data (also in Figure 3)
211 are dictated to the model as input.
212 As the transport boundary conditions, hydrographic (salinity and temperature) data is used. For
213 Northern boundary conditions, the data given in Figure 4a and 4b are used, whereas the data
214 presented in Figure 4c and 4d are adopted for Southern boundary conditions.
215 The initial conditions value of four model parameters were needed to be defined, which were
216 water level, velocity, salinity, and temperature. In the model, the initial water level and velocity
217 values are assumed as 0, termed as "Cold Start". This means that the boundary conditions will
218 determine the flow structure of the model substantially. As salinity and temperature, average values
219 of Figure 4 are adopted. For instance, average values of Figure 4a and 4c, give us a representative
220 salinity data for the whole domain. In the same way, the mean values of Figure 4b and 4d, conceive
221 initial temperature values.
222 In order to calibrate the model by flowrates, two different techniques are used in addition to the
223 manual calibration: 1) gradient based Levenberg Marquardt [36] [37] [38] 2) Covariance Matrix
224 Adaptation Evolution Strategy (CMA-ES) [39] [40]. Levenberg-Marquardt (LM) method finds the
225 local best solution, whereas CMA-ES is a global metaheuristic search algorithm.

226 **3. Results**

227 Before the calibration process, the most sensitive parameters that affect the model results are
228 determined using one-at-a-time local sensitivity analysis method based on Jacobian matrix in PEST
229 toolbox [36]. Initially, number of calibration parameter candidates were 17. These parameters are
230 Manning Roughness Coefficient; Horizontal and Vertical Eddy Viscosities; Horizontal and Vertical

Eddy Diffusivities; Wind Stress Coefficients A, B and C; Wind Speed Coefficients A, B and C; Secchi Depth; Stanton and Dalton Numbers; Slope in log-log Turbulence spectrum; Prandtl-Schmidt Number; and Spatial low-pass filter coefficient. Relative sensitivity values of these parameters, evaluated by Levenberg-Marquardt Method, are given in Table 1. According to this sensitivity analysis, Spatial Low-Pass Filter Coefficient, Horizontal Eddy Viscosity, Prandtl-Schmidt Number, Slope in log-log Spectrum, and Manning Roughness Coefficient are the parameters on which the model results have the highest sensitivity. Therefore, these 5 parameters are selected for the model calibration using LM and CMA-ES methods.

Table 1. Sensitivity analysis results using PEST tool [37] [38]

Parameter	Normalized Sensitivity Index	Sensitivity Level
Manning Roughness Coefficient	0.1696	Medium
Horizontal Eddy Viscosity	0.5352	High
Horizontal Eddy Diffusivity	0.0122	Low
Vertical Eddy Viscosity	0.0195	Low
Vertical Eddy Diffusivity	0.0975	Low
Wind Stress Coefficient A	0.0073	Low
Wind Speed Coefficient A	0.0052	Low
Wind Stress Coefficient B	0.0975	Low
Wind Speed Coefficient B	0.0975	Low
Wind Stress Coefficient C	0.0975	Low
Wind Speed Coefficient C	0	Low
Secchi Depth	0	Low
Stanton Number	0	Low
Dalton Number	0	Low
Slope in log-log Spectrum	0.2869	Medium
Prandtl-Schmidt Number	0.5188	High
Spatial Low-Pass Filter Coefficient	1.0000	Highest

After the sensitivity analysis, important parameters are selected and calibrated as shown in Table 2.

Table 2 shows that, PEST-LM yielded the most realistic value as far as the Manning roughness coefficient is concerned. For the Istanbul Strait, having a non-vegetated naturally formed seabed, a textbook guess for the Manning roughness coefficient would be around 0.025-0.035 [41]. While 0.02 is quite below this expected range, the value calibrated by PEST-LM method successfully captures this range.

Table 2. Calibrated values of the model parameters using three methods

Parameter	Manual	PEST-LM	CMA-ES
Manning Roughness Coefficient	0.02	0.0304	0.023
Horizontal Eddy Viscosity (m^2/s)	1	9.8598	10
Slope in log-log Spectrum	-5/3	-1.6390	-1.6667
Prandtl-Schmidt Number	0.7	0.8087	0.7
Spatial Low-Pass Filter Coefficient	0.3	0.2950	0.3333

Likewise for the horizontal eddy viscosity, a value around at the order of 10 m^2/s is much more realistic than value around 1 m^2/s, considering the mesh (grid) size adopted in the present study is at the order of hundreds to thousands of meters, and the enhanced resistance due to sub-grid turbulence should be accounted for in the horizontal eddy viscosity value.

When it comes to the other calibration parameters given in Table 2, the values achieved by all the three methods are not radically different from each other, also close to the values given in the

literature. To sum up, among the three methods employed, PEST-LM proved to yield the most physically consistent values for all the parameters.

Flowrates calculated by the model were extracted as model output in the sections which are located in the Northernmost and the Southernmost parts of the Strait. To test the reliability of the flowrate results of the model, ensemble-averaged monthly mean flowrate measurements for each month from 1999 to 2010 were taken into consideration as shown in Table 3 [21]. In this table, lower layer flowrate values directed to North are shown as negative while velocity vectors of Southward flow in the upper layer are assumed as positive.

Table 3. The average of 10 years in-situ flowrate values which are measured in North and South of the Strait [21].

Months	Upper Layer Flowrate North (m^3/s)	Lower Layer Flowrate North (m^3/s)	Upper Layer Flowrate South (m3/s)	Lower Layer Flowrate South (m3/s)
January	*8950*	*-10030*	*9150*	*-9720*
February	*14260*	*-5810*	*16080*	*-5520*
March	*15320*	*-6860*	*16190*	*-6240*
April	*16510*	*-4930*	*19150*	*-4860*
May	*16610*	*-5050*	*18410*	*-4980*
June	*15740*	*-5530*	*17590*	*-5730*
July	*12510*	*-7830*	*12210*	*-8220*
August	*12670*	*-8300*	*13890*	*-8270*
September	*9000*	*-10190*	*9060*	*-9960*
October	*8030*	*-13000*	*7880*	*-12010*
November	*9950*	*-9330*	*9210*	*-9100*
December	*14240*	*-8410*	*14800*	*-8730*
Average	*8950*	*-10030*	*9150*	*-9720*

3.1. Hydrodynamic Model Calibration

In this study, the monthly average flowrate values (from January to December) computed by the numerical model are compared with the ensemble-averaged monthly mean values of the 10 years in-situ observations. Figure 7 and 8 show the modeled and observed monthly average flowrate for the lower and upper layers at the Northern and Southern part of the Strait.

When Figure 7 and 8 are investigated, it can apparently be seen that the Levenberg-Marquardt calibration algorithm (PEST-LM) is the best fitting method generally [36] . Especially in the Northern part of the Strait, agreement of PEST-calibrated model output with the observed values is remarkable. On the other hand, PEST-LM method cannot said to be the most efficient method for calibration. When it comes to the South station measurements, manual calibration and CMA-ES performed slightly better than the PEST-LM method.

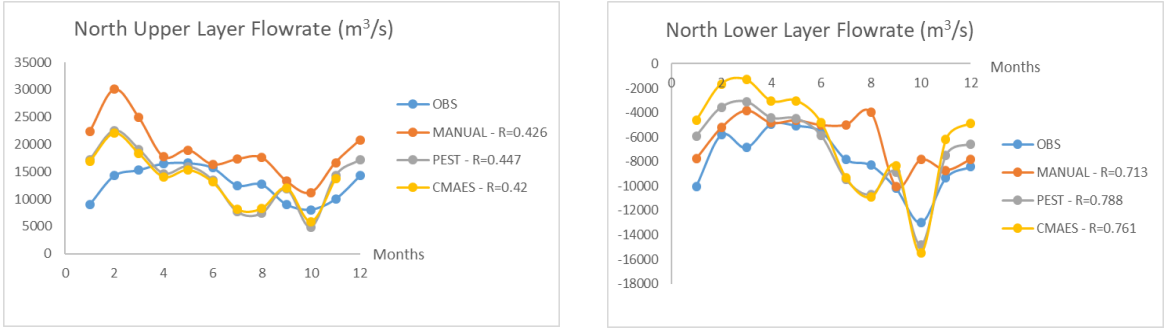

(a) *(b)*

Figure 7. Upper (a) and Lower (b) Flowrate values of Northern Part of the Strait

Preprints (www.preprints.org) | NOT PEER-REVIEWED | Posted: 28 August 2019 doi:10.20944/preprints201908.0299.v1

Peer-reviewed version available at Processes 2019, 7, 710; doi:10.3390/pr7100710

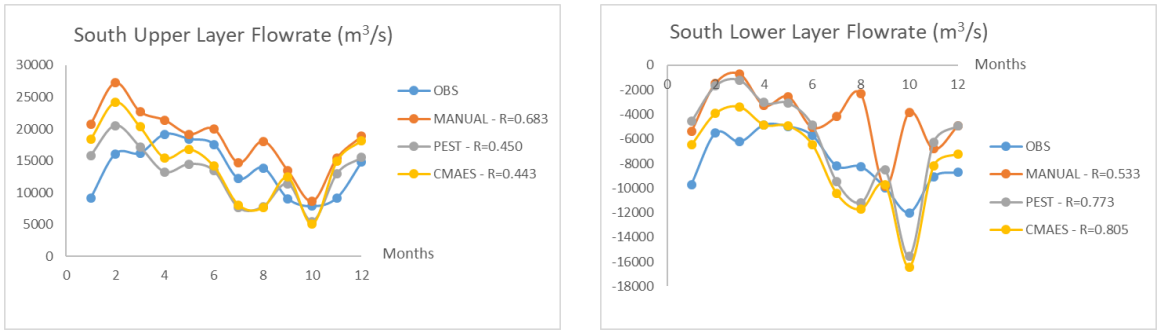

(a) *(b)*

Figure 8. Upper (a) and Lower (b) Flowrate values of Southern Part of the Strait

According to Figure 7 and 8, it is understood that, observations and modeled flowrates are in accordance generally. One can easily see that North and South flowrates are not the same. This difference between flowrates originates from the mixing taking place between the lower and upper flow layers. For instance, a water element travelling from the Marmara Sea through the lower layer Northwards tend to entrain to the upper layer in hydraulic control sections. As mentioned before, these sections are the locations of most significant vertical mixing flows in the Strait. This mass transfer between the two layers introduces the differences between flowrates recorded at the North and South sections.

3.2 Hydrographic Model Validation

As mentioned above, the model is calibrated according to monthly average flowrate values. Although the performance of the calibration process was shown to be satisfactory, calibration alone is not always sufficient to prove the reliability of the model. To validate the model in a robust way, salinity and temperature processes profiles along the Strait are also examined. Figure 9 presents the longitudinal salinity profiles of the Istanbul Strait for four different months, namely January, April, July, and October. According to this figure, dispersion and distribution of salinity in the model substantially agrees with the in-situ observations. Stratification in the Strait clearly reveals itself in salinity profiles, such that the upper and lower flow layers can easily be distinguished. Normally, upper zones are less saline, around 18-20 ppt, and deeper zones are more saline, around 38-40 ppt. This is because, the upper layer originates from Black Sea fed by less saline sources such as the Danube River, while the source of the lower layer is saline waters of Marmara, Aegean, and Mediterranean Seas. It can be seen from the model results as well as observations that when the flowrate of the upper layer increases, thickness of this layer with the less saline water mass (blue in the figures) also increases.

300

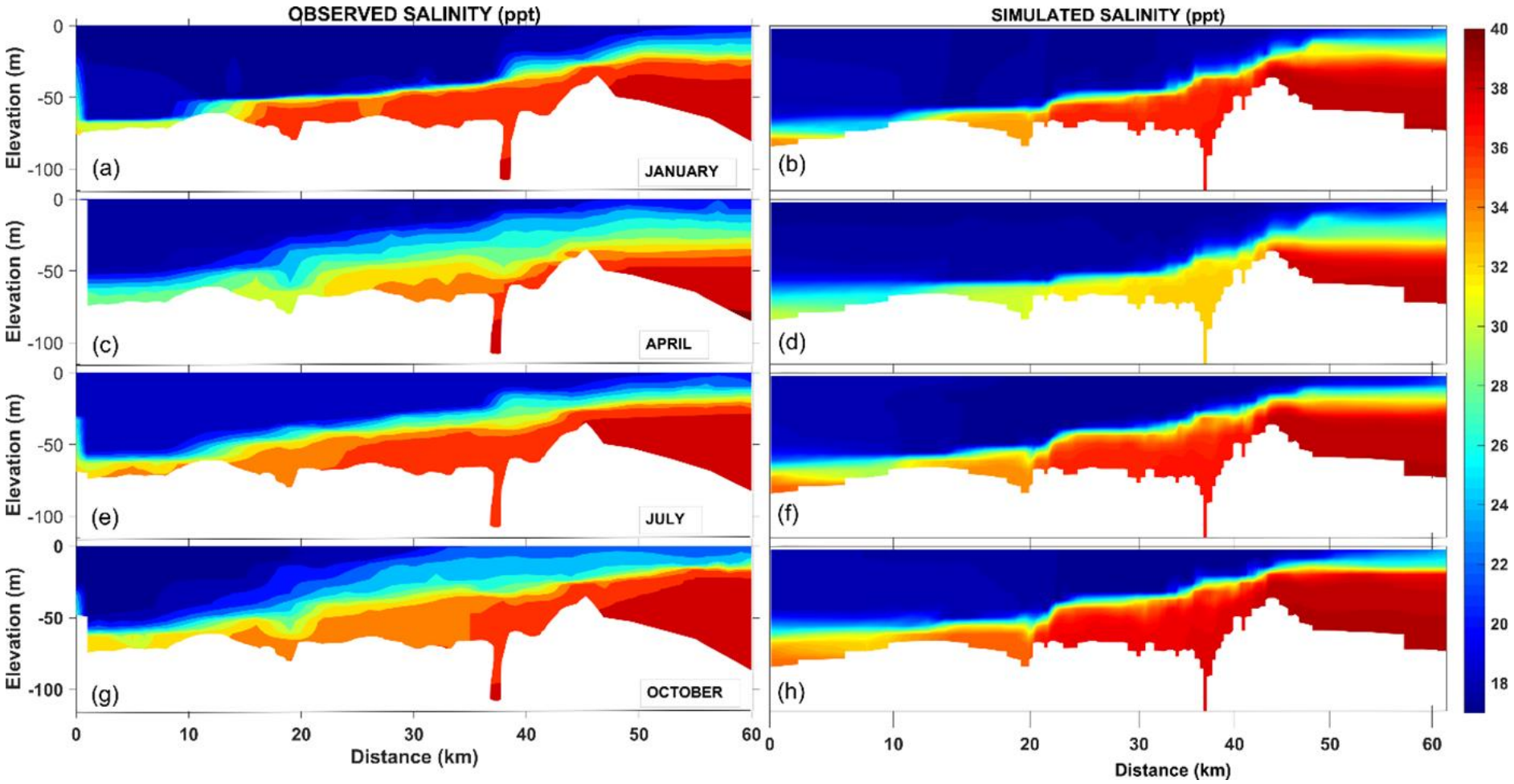

301

302 **Figure 9.** Salinity profiles of observed (a) and modeled (b) in January, observed (c) and modeled (d) in April, observed (e) and modeled (f) in July, and observed (g) and
303 modeled (h) in October.

304
305 Another conspicuous feature of the Strait is the variation seawater temperature in vertical.
306 Figure 10 gives the longitudinal temperature profiles of the Strait, respectively in January, April, July,
307 and October. This figure also involves the model results as well as the measured temperature profiles.
308 The most imperative feature of the Strait, stratification, is also clearly represented by the numerical
309 model from the temperature viewpoint. Although a general agreement between the model results
310 and the measured data can be assessed, it is seen that the performance of the numerical model for
311 modelling the temperature profiles is not as effective as the salinity modeling. The potential reason
312 is that more complicated atmospheric effects (such as atmospheric cooling and warming) are engaged
313 in the temperature modeling on the contrary of salinity, which is mostly governed by the
314 oceanographic/mareographic parameters. Nevertheless, the profiles of the stratified temperature
315 structure can generally said to be captured by the numerical model results, even though it is not as
316 accurate as salinity profiles. For instance, in January and April, upper layer is colder than lower layer,
317 and in the July and October vice versa. Both conditions are exhibited in the numerical model within
318 a fair approximation. A visible drawback in the model is that, thickness of the intermediate layer
319 could not always be properly modeled. Especially in the July results, this defect is observed.
320 Irrespective of the drawback, it can be said that observed temperature profiles are modelled with a
321 fair agreement.
322

323

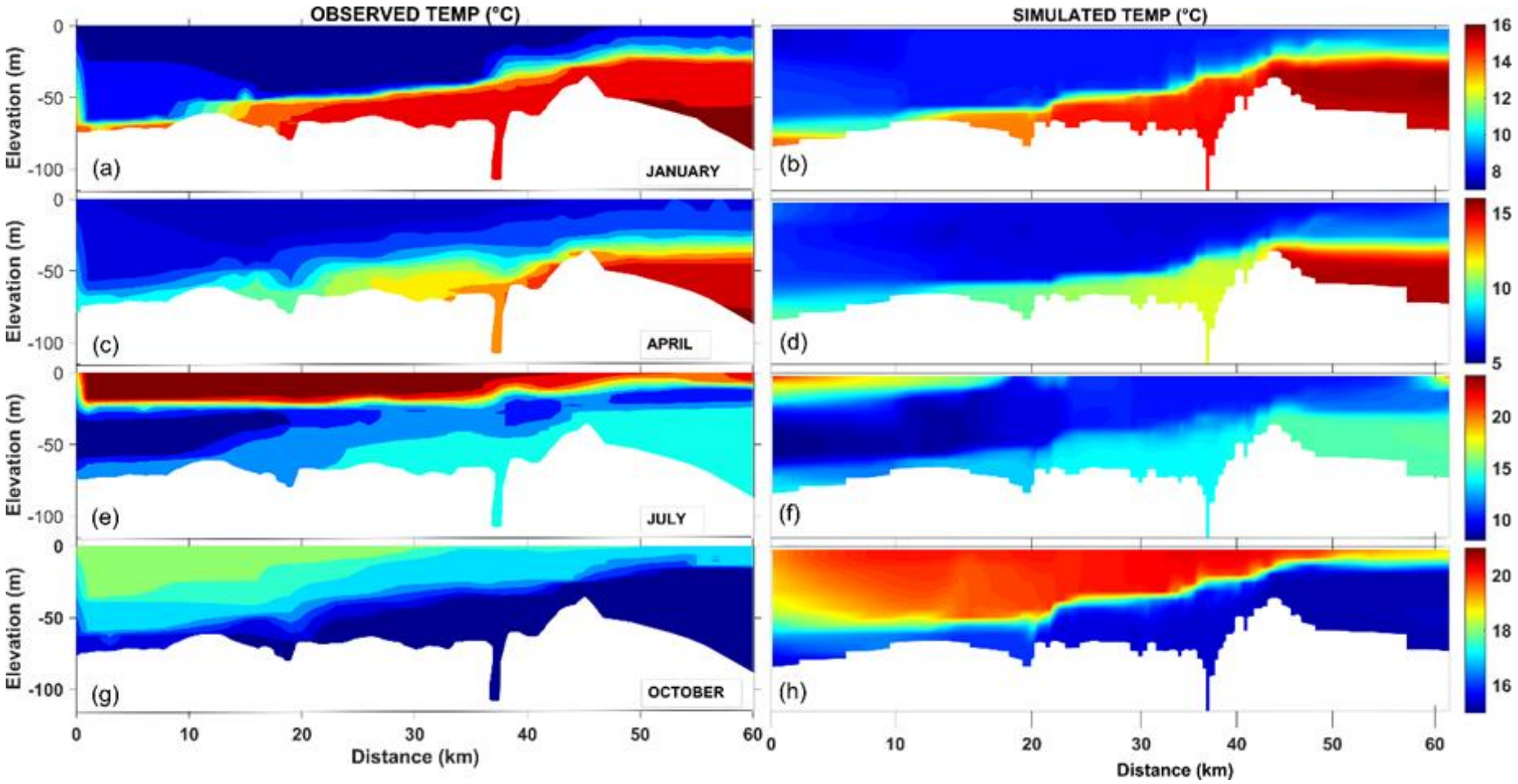

324

325 Figure 10. Temperature profiles of observed (a) and modeled (b) in January, observed (c) and modeled (d) in April, observed (e) and modeled (f) in July, and observed (g)
326 and modeled (h) in October.

4. Discussion

In this study, Istanbul Strait, one of the most complicated waterways in the world with its meandering shape, stratified structure, and hydraulic control process, is numerically modelled. The main objective of the study is to model the hydrodynamic and hydrographic constitution of the Strait, as well as assessing the most sensitive hydrodynamic parameters to reach a successful solution.

Three different methods are employed for calibration of the model by comparing the in-situ measured flowrates of upper and lower layers at the North and South parts of the Strait with the numerical model results. Among the employed methods, Levenberg-Marquardt Algorithm (PEST method) came out to be the best to calibrate the model, not only due to the closest agreement between the measurements and the model, but also with the physically consistent values of the input parameters attained as the end-product of the calibration process. With the mentioned method used, correlation between numerical model results and observations got higher. Especially in the Northern section of the Strait, the method was perceptibly successful.

Sensitivity analysis showed that among the 17 input parameters, the following five has the most prominent effect on the results: (1) Spatial Low-Pass Filter Coefficient, (2) Horizontal Eddy Viscosity, (3) Prandtl-Schmidt Number, (4) Slope in log-log Spectrum, and (5) Manning Roughness Coefficient.

Apart from the flowrate results of the upper and lower layers, salinity and temperature profiles of the stratified flow in the Strait were assessed by the numerical model, in comparison with the in-situ measurements. This latter comparison served as a means of validation of the numerical model. Modeled salinity profiles came out to be another prospering output of this study. Beside the stratification of the Strait, salinity values and layer thicknesses are modeled in good agreement with the measurements, such that modeled and observed salinity profiles closely resembled each other. When it comes the temperature profiles, stratification and seasonality variations were seen to be fairly represented in the numerical model results. Although the thickness of the intermediate cold layer was not accurately estimated by the model results, general temperature profiles of the model were seen to be in accord with observed profiles. Choosing calibration and validation dataset very different is one of the unique feature of our study. Obviously if the calibration framework includes the observed temperature as part of the objective function, the model simulation performance on temperature profiles will substantially increase. This is an ongoing modelling effort and will be the topic of a subsequent study.

With this numerical modelling study, it was clearly seen that the robustness of the model is depending on the sufficient representation of the boundary and initial conditions, as well as the accurate water level inputs which are the main forcing factor of the flow. Stratification phenomena can only be modeled with properly assigning the stratified boundary and initial conditions, as was done in the present study.

In future studies, temporal and spatial domains of the model could be extended in order to model the Strait in a more proper way, preferably with a higher grid resolution. As such, the agreement of hydrodynamic and hydrographic outputs between model and the observations could get better in these future studies, with which estimations on the effect of climate change on the delicate flow regime of the Istanbul Strait can possibly be modelled.

Author Contributions: conceptualization, M.M.K. and M.C.D.; methodology, M.M.K. and M.C.D.; software, M.M.K. and M.C.D.; validation, M.M.K., M.C.D. and V.S.O.K.; formal analysis, M.C.D. and V.S.O.K.; investigation, M.M.K. and V.S.O.K.; resources, M.M.K. and V.S.O.K.; data curation, M.M.K. and M.O.; writing—original draft preparation, M.M.K., M.C.D., V.S.O.K and M.O.; writing—review and editing, M.C.D. and V.S.O.K.; visualization, M.M.K., M.C.D. and V.S.O.K.; supervision, M.O.

Funding: This research was funded by Istanbul Technical University, grant number 38420. The second author (MCD) is supported by Turkish Scientific and Technical Research Council (TÜBİTAK grant 118C020)

References

1. Çeçen, K.; Bayazıt, M.; Sümer, M.; Güçlüer, Ş.; Doğusal, M.; Yüce, H. *İstanbul Boğazı'nın Hidrolik ve Oşinografik Etüdü (The Hydraulic and Oceanographic Survey of Istanbul Strait)*; Istanbul Technical University: Istanbul, 1981;

2. Bayazıt, M.; Sümer, M. İstanbul Boğazı'nın Hidrolik ve Oşinografik Etüdü - 2 (The Hydraulic and Oceanographic Survey of Istanbul Strait - 2).pdf 1982, 23.

3. Sumer, B.M.; Bakioglu, M. Sea-Strait Flow With Special Reference To Bosphorus. **1981**.

4. Latif, M.A.; Özsoy, E.; Oguz, T.; Ünlüata, Ü. Observations of the Mediterranean inflow into the Black Sea. *Deep Sea Res. Part A. Oceanogr. Res. Pap.* **1991**, *38*, S711–S723.

5. Özsoy, E.; Beşiktepe, Ş.; Latif, M.A. Türk Boğazlar Sistemi'nin Oşinografisi (Oceanography of the Turkish Strait System). **2000**.

6. Falina, A.; Sarafanov, A.; Özsoy, E.; Utku Turunçoğlu, U. Observed basin-wide propagation of Mediterranean water in the Black Sea. *J. Geophys. Res. Ocean.* **2017**, *122*, 3141–3151.

7. Sur, H.I.; Özsoy, E.; Ünlüata, Ü. Boundary current instabilities, upwelling, shelf mixing and eutrophication processes in the Black Sea. *Prog. Oceanogr.* **1994**, *33*, 249–302.

8. Oguz, T.; Özsoy, E.; Latif, M.A.; Sur, H.I.; Ünlüata, Ü. Modeling of Hydraulically Controlled Exchange Flow in the Bosphorus Strait. *J. Phys. Oceanogr.* **1990**, *20*, 945–965.

9. Farmer, D.M.; Armi, L. Maximal two-layer exchange over a sill and through the combination of a sill and contraction with barotropic flow. *J. Fluid Mech.* **1986**, *164*, 53–76.

10. Armi, L.; Farmer, D.M. Maximal two-layer exchange through a contraction with barotropic net flow. *J. Fluid Mech.* **1986**, *164*, 27–51.

11. Armi, L. The hydraulics of two layers with different densities. *J. Fluid Mech.* **1986**, *163*, 27–58.

12. Dorrell, R.M.; Peakall, J.; Sumner, E.J.; Parsons, D.R.; Darby, S.E.; Wynn, R.B.; Özsoy, E.; Tezcan, D. Flow dynamics and mixing processes in hydraulic jump arrays: Implications for channel-lobe transition zones. *Mar. Geol.* **2016**, *381*, 181–193.

13. Beşiktepe, Ş.T.; Sur, H.I.; Özsoy, E.; Latif, M.A.; Oğuz, T.; Ünlüata, Ü. The circulation and hydrography of the Marmara Sea. *Prog. Oceanogr.* **1994**, *34*, 285–334.

14. Ozsoy, E.; Latif, M.A.; Besiktepe, S.; Çetin, N.; Gregg, M.C.; Belokopytov, V.; Goryachkin, Y.; Diaconu, V. The Bosporus Strait: Exchange Fluxes, Currents and Sea-Level Changes. *Nato Sci. Ser. 2 Environ. Secur.* **1998**, *47*, 1–28.

15. Gregg, M.C.; Özsoy, E.; Latif, M.A. Quasi-steady exchange flow in the Bosphorus. *Geophys. Res. Lett.* **1999**, *26*, 83–86.

16. Gregg, M.C.; Özsoy, E. Flow, water mass changes, and hydraulics in the Bosphorus. *J. Geophys. Res.* **2002**, *107*.

17. Güler, I.; Yüksel, Y.; Yalçiner, A.C.; Çevik, E.; Ingerslev, C. Measurement and evaluation of the hydrodynamics and secondary currents in and near a strait connecting large water bodies-A field study. *Ocean Eng.* **2006**, *33*, 1718–1748.

18. Yuksel, Y.; Ayat, B.; Nuri Ozturk, M.; Aydogan, B.; Guler, I.; Cevik, E.O.; Yalçiner, A.C. Responses of the stratified flows to their driving conditions-A field study. *Ocean Eng.* **2008**, *35*, 1304–1321.

19. Aydoğan, B.; Ayat, B.; Öztürk, M.N.; Özkan Çevik, E.; Yüksel, Y. Current velocity forecasting in straits with artificial neural networks, a case study: Strait of Istanbul. *Ocean Eng.* **2010**, *37*, 443–453.

20. Jarosz, E.; Teague, W.J.; Book, J.W.; Beşiktepe, Ş. Observed volume fluxes in the Bosphorus Strait. *Geophys. Res. Lett.* **2011**, *38*, n/a-n/a.

21. Altiok, H.; Kayişoğlu, M. Seasonal and interannual variability of water exchange in the Strait of Istanbul. *Mediterr. Mar. Sci.* **2015**, *16*, 644–655.

22. Ozsoy, E.; Cagatay, M.N.; Balkis, N.; Balkis, N.; Ozturk, B. *The Sea of Marmara - Marine Biodiversity, Fisheries, Conservation and Governance*; 2016; ISBN 9789758825349.

23. Akay, O. Hydrodynamic Simulation of the Bosphorus, Istanbul Technical University, Institute of Science and Technology, 2002.

24. Öztürk, M.N. İstanbul Boğazı'nın Hidrodinamiği ve Sayısal Modellenmesi (Hydrodynamics of the Istanbul Strait and its Numerical Model), Yildiz Technical University, 2010.

25. Sözer, A. Numerical Modeling of the Bosphorus Exchange Flow Dynamics, Middle East Technical University, 2013.

26. Sözer, A.; Özsoy, E. Modeling of the Bosphorus exchange flow dynamics. *Ocean Dyn.* **2017**, *67*, 321–343.

27. Sannino, G.; Sözer, A.; Özsoy, E. *A high-resolution modelling study of the Turkish Straits System*; Ocean Dynamics, 2017; Vol. 67; ISBN 1023601710.

28. Armi, L.; Farmer, D.M. The Internal Hydraulics of the Strait of Gibraltar and Associated Sills and Narrows. *Oceanol. Acta* **1985**, *8*, 37–46.

29. Bruno, M.; Chioua, J.; Romero, J.; Vázquez, A.; Macías, D.; Dastis, C.; Ramírez-Romero, E.; Echevarria, F.; Reyes, J.; García, C.M. The importance of sub-mesoscale processes for the exchange of properties through the Strait of Gibraltar. *Prog. Oceanogr.* **2013**, *116*, 66–79.

30. Koşucu, M.M. Three-Dimensional Hydrodynamic Model of the Istanbul Strait, Istanbul Technical University, Institute of Science and Technology, 2016.

31. Sur, H.İ.; Okuş, E.; Güven, K.; Yüksek, A.; Altiok, H.; Kıratlı, N.; Ünlü, S.; Taş, S.; Aslan Yılmaz, A.;

Yılmaz, N.; et al. *Water Quality Monitoring: Annual Report (2003)*; Istanbul, 2004;

32. Delft3D user manual Simulation of multi-dimensional hydrodynamic flow and transport phenomena, including sediments 2014, 684.

33. Cornelissen, S. Numerical Modelling of Stratified Flows Comparison of the σ and z coordinate systems. **2004**, 1–94.

34. Lesser, G.R.; Roelvink, J.A.; van Kester, J.A.T.M.; Stelling, G.S. Development and validation of a three-dimensional morphological model. *Coast. Eng.* **2004**, *51*, 883–915.

35. Huang, W.; Spaulding, M. Modeling horizontal diffusion with sigma coordinate system. *J. Hydraul. Eng.* **1996**, *122*, 349–356.

36. Doherty, J. *PEST: Model Independent Parameter Estimation. Fifth Edition of User Manual*; Watermark Numerical Computing: Brisbane, 2005;

37. Doherty, J. *Calibration and Uncertainty Analysis for Complex Environmental Models*; Watermark Numerical Computing: Brisbane, Australia, 2015; ISBN 978-0-9943786-0-6.

38. Doherty, J. *Model-Independent Parameter Estimation(Part I)*; 6th ed.; Watermark Numerical Computing, 2016;

39. Hansen, N.; Ostermeier, A. Completely derandomized self-adaptation in evolution strategies. *Evol. Comput.* **2001**, *9*, 159–195.

40. Hansen, N.; Ostermeier, A. Adapting arbitrary normal mutation distributions in evolution strategies: the covariance matrix adaptation.; 2002.

41. Dey, S. *Fluvial hyrodynamics: Hydrodynamic and sediment transport phenomena*; Springer: Berlin, Germany, 2014; ISBN 978-3-642-19061-2.